ACS APPLIED MATERIALS & INTERFACES

Research Article

www.acsami.org

Surface Modification of Bacterial Cellulose Aerogels' Web-like Skeleton for Oil/Water Separation

Huazheng Sai,[†] Rui Fu,[†] Li Xing, Junhui Xiang,* Zhenyou Li, Fei Li, and Ting Zhang

College of Materials Science & Optoelectronic Technology, University of the Chinese Academy of Sciences, Yuquan Road 19A, Beijing 100049, China

Supporting Information

ABSTRACT: The cellulose nanofibers of bacterial cellulose aerogel (BCA) are modified only on their surfaces using a trimethylsilylation reaction with trimethyichlorosilane in liquid phase followed by freeze-drying. The obtained hydrophobic bacterial cellulose aerogels (HBCAs) exhibit low density ($\leq$6.77 mg/cm^3), high surface area ($\geq$169.1 m^2/g), and high porosity ($\approx$ 99.6%), which are nearly the same as those of BCA owing to the low degrees of substitution ($\leq$0.132). Because the surface energy of cellulose nanofibers decreased and the three-dimensional web-like microstructure, which was comprised of ultrathin (20−80 nm) cellulose nanofibers, is maintained during the trimethylsilylation process, the HBCAs have hydrophobic and oleophilic properties (water/air contact angle as high as 146.5°) that endow them with excellent selectivity for oil adsorption from water. The HBCAs are able to collect a wide range of organic solvents and oils with absorption capacities up to 185 g/g, which depends on the density of the liquids. Hence, the HBCAs are wonderful candidates for oil absorbents to clean oil spills in the marine environment. This work provides a different way to multifunctionalize cellulose aerogel blocks in addition to chemical vapor deposition method.

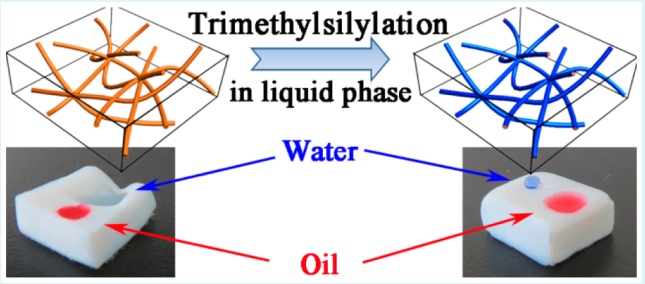

KEYWORDS: *surface modification, bacterial cellulose, aerogels, liquid phase, oil−water separation*

INTRODUCTION

With increasing offshore oil production and transportation, oil and various petroleum products spillage and leakage at sea are becoming more and more frequent.[1−4] These accidents (e.g., the Gulf of Mexico oil spill accident in 2010) can cause natural disasters that have significant impact on the environment and wildlife. Hence, cleaning oil spills under the marine environment is an urgent and challenging task.[5−13] Generally, current strategies are classified into three groups: extracting the oil from water surface; dispersing the oil in water by applying dispersant agents to facilitate nature degradation; and burning the oil spill in situ.[14−16] Among these, collection of oil from water with sorbents is considered as one of the most promising approaches due to the convenience of this method, which allows proper disposal of the oil and does not create secondary pollution.[17−25] Thus, it is vital to choose the appropriate material as the oil absorbents for this method.[26−28] The sorbent should exhibit high oil absorption capacity, high oil/water selectivity, high uptake rate, high floatability (i.e., low density), low cost, environmental friendliness, and potential recyclability.

The traditional oil sorption materials can be categorized into three major classes: mineral products[29−31] (e.g., zeolites, sepiolite, and expanded perlite), natural materials[32−34] (e.g., cotton, wooden chips, wool, silkworm cocoon waste, and vegetable fibers) and synthetic polymers[35−37] (e.g., rubber, commercial polypropylene fiber mats, electrospun fibrous film, and electrospun polystyrene−polyurethane fibrous mats and polyurethane foam). However, mineral products and natural materials exhibit poor buoyancy, low sorption capacity, and poor oil/water selectivity and are inconvenient to recycle. Even though the sorption capacity and oil/water selectivity are significantly higher than those of the two former materials, the polymers degrade much more slowly, and their environmental and ecological impact remains unclear. These drawbacks of the traditional oil sorbents and the demand of novel, efficient, and green materials drive the research community to find better alternatives.

Aerogels as oil/water separation materials have drawn significant attention owing to their low density, large specific surface area, and large porosity.[16,38,39] However, traditional inorganic aerogels (e.g., silica aerogels) are too brittle for utilization.[40] Although various new carbon-based aerogels[41,42] based on carbon nanotube and graphene exhibit very high sorption capacities and good recyclability, the expensive equipment and complex technologies involved in their manufacture restrict their practical applications. Hence, researchers endeavor to explore new aerogel materials with excellent properties and low cost for oil/water separation.

Recently, the novel cellulose aerogels (also designated as cellulosic sponges or foam in the literature) based on

Received: January 28, 2015
Accepted: March 23, 2015
Published: March 23, 2015

DOI: 10.1021/acsami.5b00846
ACS Appl. Mater. Interfaces 2015, 7, 7373−7381

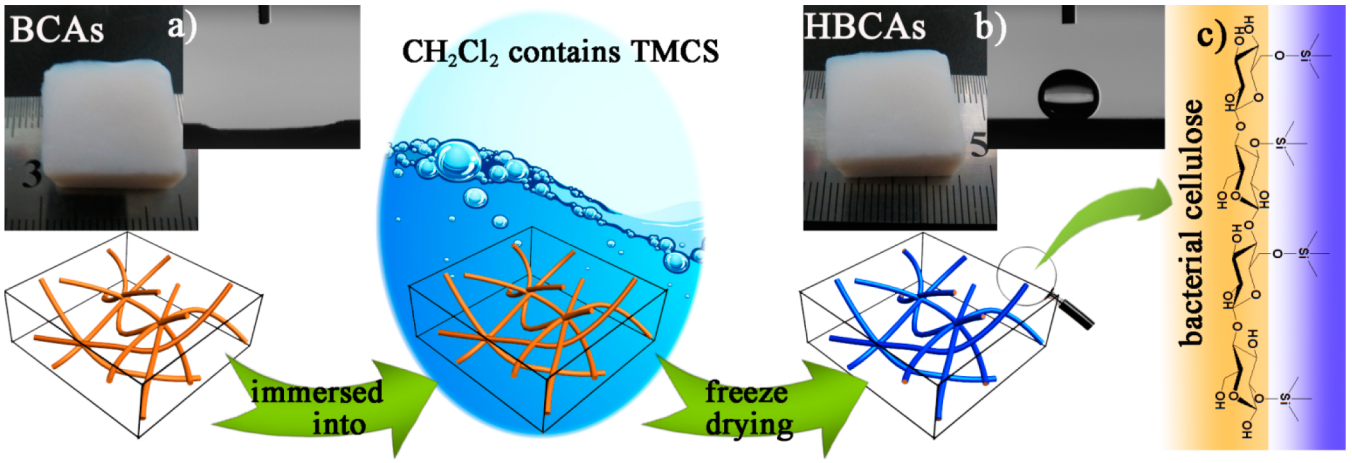

Figure 1. Schematic illustration of the trimethylsilylation of BCAs. (a) The image and contact angle test of BCA. (b) The image and contact angle test of HBCA. (c) The schematic chemical structure of modified bacterial cellulose.

nanofibrillated cellulose (NFC) have aroused a wide research interests due to their renewability, good mechanical properties, low density, high porosity, natural biodegradability, and environmental friendliness.[43−47] These fascinating properties make it possible to used them as oil sorbents.

As ideal oil sorbents, cellulose aerogels have to be tailored to convert the inherent hydrophilicity of aerogel skeleton to hydrophobicity and oleophilicity to make sure that they can exhibit excellent oil/water selectivity. In recent years, the cellulose aerogels are mostly hydrophobization modified directly via gas phase reactions. Ikkala et al.[15,48] functionalized the native nanocellulose aerogels with a nanoscopic layer of titanium dioxide (TiO_2) to create a hydrophobic but oleophilic coating by chemical vapor deposition (CVD). Cervin et al.[49] treated the hydrophilic cellulose aerogels with octyltrichlorosilane through vapor phase deposition. Similarly, Heux et al.[50,51] made the vapor of palmitoyl chloride diffused into the void of cellulose aerogels to initiate the esterification with the hydrophilic hydroxyl in cellulose, while they did not discuss the oil/water separation properties in the literature. The preparation conditions (i.e., reaction temperature, vapor pressure, reaction time and the initial quantity of reagent) of the gas phase reactions need to be controlled accurately. In fact, the strict preparation conditions hamper the large-scale production of these hydrophobic cellulose aerogels for practical application. Moreover, the grafting distribution within the material is not homogeneous. Very recently, to solve these problems, Tingaut et al.[14] prepared the hybrophobic cellulose aerogels by freeze-drying water suspensions of NFC in the presence of methyltrimethoxysilane (MTMS) sols. However, the microstructure and some properties of the cellulose aerogels may be remarkably affected by the silylation agent (i.e., MTMS) during this process.

In this study, we attempted to find a feasible way to conformally modify the 3D web-like skeleton of cellulose aerogels in liquid phase without CVD. Although many reports have shown how cellulose was hydrophobilized in liquid phase, to the best of our knowledge, all of them were focus on tailoring the properties of the disperse cellulose nanofibers, not the monolithic cellulose aerogels, because the hydrophobization of cellulose nanofibers could enhance their dispersibility in nonpolar media (e.g., organic solvents) and the compatibility between cellulose and hydrophobic polymer.[52−57] Here, we immersed blocky bacterial cellulose aerogel (BCA) in organic solvent which contain trimethylchlorosilane (TMCS) to trimethylsilylate the 3D web-like skeleton of BCA, followed by freeze-drying to obtain the intact hydrophobic bacterial cellulose aerogels (HBCAs; Figure 1). Compared with CVD method,[15,48−51,58] the modifier which has uniformly dispersed in liquid could diffuse into the pore with the dispersant rapidly. This process makes sure all the cellulose nanofibers in the aerogels are in the same reaction environment and then avoid the heterogeneity in the obtained materials by the CVD method. Furthermore, unlike the vapor with modifiers will take much time to diffuse into the inner of the cellulose aerogels when the size of the aerogels is large, the size of cellulose aerogels will not affect the diffusion time of modifiers obviously in this work. It is also different from the method reported by Tingaut et al.[14] that the modifier could sol−gel among the cellulose network and alter the microstructure obviously. In this work, as the facile modification only occurred on the surface of the bacterial cellulose nanofibers, the micromorphology of BCA is unchanged. Hence, similar to BCA, HBCA are ultralight (density ≤6.77 mg/cm^3), highly porous (porosity, ≈99.6%), and have a surface area over 169.1 m^2/g. Moreover, the HBCAs have hydrophobic and oleophilic properties that endow them with an excellent selectivity for oil adsorption from water. The HBCAs could collect a wide range of oils and organic solvents and showed the absorption capacities of up to 185× their own weight, which depended on the density of the liquids.

EXPERIMENTAL SECTION

Materials. The foodstuff nata de coco (bacterial cellulose hydrogel) was procured from Kuangquan Food Co., Ltd. (Tangshan, China). TMCS (≥98%) and triethylamine (TEA, ≥99%), paraffin liquid, and chlorobenzene (≥99%) were purchased from Sinopharm Chemical Reagents Co., Ltd. (Shanghai, China). Dichloromethane (CH_2Cl_2, ≥99.5%), ethanol (≥99.7%), *n*-hexane (≥95%), toluene (≥99.5%), and acetone (≥99.5%) were bought from Beijing Chemical Reagents Co. (Beijing, China). *tert*-Butanol was produced by Tianjin Fuchen Chemical Reagents Factory (Tianjin, China). Gasoline and diesel were obtained from Sinopec Corp. All chemicals and solvents were used as received without further purification. Deionized water was used in all experiments.

Preparation of BCAs. The pure BCAs were prepared from nata de coco (i.e., bacterial cellulose hydrogel) directly via freeze-drying according to a procedure previously published by our group.[59] The bacterial cellulose hydrogel was immersed in deionized water (4 h) to wash out the sugar. The washed bacterial cellulose hydrogel was

DOI: 10.1021/acsami.5b00846
ACS Appl. Mater. Interfaces 2015, 7, 7373−7381

heated to 90 °C in a concentrated NaOH solution (6 h), then washed with deionized water (10 h), followed by replacement of the deionized water with a mixture of deionized water and *tert*-butanol, and then freeze-dried to preserve the web-like structure of the bacterial cellulose in the dry state.

Synthesis of HBCAs. First, different amounts (Table 1) of TMCS and TEA were mixed with 30 mL dichloromethane in a 100 mL round-bottom flask, stirring constantly (200 rpm) with a magnetic stirrer. Then, BCA (ca. 0.03 g) was added to the flask and keep stirring. The reflux apparatus was assembled and the flask was secured to it. Heat the flask (60 °C) to make the mixture reflux for 4 h. Next, the cellulose blocks were put in a beaker with 50 mL ethanol, and kept stirring constantly to wash dichloromethane, residual reactants and byproducts (triethylamine hydrochloride) out from the void of the 3D web-like cellulose skeleton. The ethanol was changed every hour.

Table 1. Amounts of Modifying Agent Used Here[a]

	BCA	HBCA-1	HBCA-2	HBCA-3
TMCS (mL)		1	2	3
TEA (mL)		1.32	2.64	3.96

[a]Washed cellulose blocks were solvent exchanged with a mixture of deionized water and *tert*-butanol. Then, the gels were precooled for 8 h at −20 °C, followed by freeze-drying for 15 h to obtain the dried HBCAs.

Fourier Transform Infrared (FTIR) Spectroscopy. The attenuated total reflection (ATR) infrared spectra of BCA and the HBCAs were obtained on a VERTEX 70 FT-IR spectrometer (Bruker, Germany). All spectra were recorded between 4000 and 400 cm^{-1} with a resolution of 4 cm^{-1} and 16 scans per sample.

Morphology and Nanostructure. Field-emission scanning electron microscopy (SEM) characterization of the aerogels was performed by a Hitachi S-4800 (Japan) at accelerating voltage of 10 kV and a working distance of 10 mm. Samples were stuck on the sample holder with a carbon pad and coated with 7.5 nm of platinum.

Energy-Dispersive X-ray (EDX) Spectra. The content of the relative elements of all the samples was determined by EDX spectra. The test conditions are the same as those used for SEM characterization, but the samples fixed on the carbon pad were thicker (>2 mm) to avoid the interference of the carbon basement. In addition, the samples were not sputtered with platinum to eliminate the extraneous platinum signals.

Contact Angle Measurements. Static contact angles of these samples were measured using the contact angle measuring system (JC2000C1, POWEREACH). A droplet (5 μL) of deionized water was deposited on the surface of the samples. At least five measurements were taken for each sample.

Density. The density of BCA and the HBCAs was determined by measuring the weight and volume of each individual sample. The weight of each aerogel block was measured by an analytical balance (readability 0.00001 g, SARTORIUS). The dimensions of each aerogel block were measured with a digital caliper at three different positions. Five blocks were used for density determination for each sample.

Porosity. The porosity (P) of BCA was calculated using the bulk density of BCA (ρ_b) and the skeleton density of cellulose aerogels (ρ_s) using eq 1, obtained from the simple rule of mixtures and assuming the gas density was negligible. Herein, the ρ_s was fixed at 1.59 g/cm^3, based on literature data.

$$P\ (\%) = \left(1 - \frac{\rho_b}{\rho_s}\right) \times 100 \tag{1}$$

Nitrogen Physisorption Measurements. First, the sample was degassed at 120 °C for 2 h. Then, the nitrogen physisorption measurements at 77 K were performed with a Gemini V (Micromeritics, Norcross, GA). Brunauer−Emmett−Teller (BET) Analysis from the amount of N_2 absorbed at various relative vapor pressures (six points $0.05 < p/p_0 < 0.3$, nitrogen molecular cross-sectional area = 0.162 nm^2) was used to determine the surface area.

Thermal Stability. The thermal degradation behavior of BCA and HBCAs in nitrogen was investigated using thermogravimetry analysis (TGA, SDT Q600). A sample weight of approximately 5 mg was used. The sample was placed in a ceramic pan and heated from 50 to 650 °C at a heating rate of 10 °C/min.

X-ray Diffraction (XRD) to Determine the Crystallinity of BCA and HBCAs. The XRD pattern of each sample was characterized by an MSAL-SD3 X-ray diffractometer (China) with Ni-filtered Cu Kα radiation (λ = 0.1541 nm) in the range of 10−40° (2θ) at 40 kV and 40 mA. All the samples were cut into about 2 mm thickness and pressed on the sample holder by a glass slide. To evaluate the crystallinity of bacterial cellulose affected by the hydrophobization, we used Segal's method. This eq 2 is an empirical equation for estimating the degree of crystallinity (χ_c) in cellulose.[60]

$$\chi_c\ (\%) = \frac{I_{200} - I_{\text{amorphous}}}{I_{200}} \times 100 \tag{2}$$

where I_{200} and $I_{\text{amorphous}}$ are the intensity of the 200 reflection plane and the amorphous phase, respectively.

The structure order of the 200 reflection was used to determine the crystallite size (L_{200}) by eq 3.[60] In this equation, β is the full width at half-maximum of the 200 reflection, θ is the Bragg's angle in degrees, and K = 0.91.

$$L_{200} = \frac{K\lambda}{\beta \cos\theta} \tag{3}$$

Mechanical Properties. The stress−strain curves of BCAs and HBCAs were measured by Istron-3365 flexural strength testing systems when all the samples were cut into the same cuboid form. The similar tests for oil-filled HBCAs were also carried out.

Oil and Organic Solvent Absorption Capacities. The samples were cut into slices (ca. 20 × 8 × 2 mm) and dipped into 10 mL of oils or organic solvents. Then, we took the swollen samples out at certain intervals to determine their weights and obtain the absorption kinetic curves and the maximum absorption capacities (C_m). C_m was calculated according to eq 4:

$$C_m\ (g/g) = (W_t - W_0)/W_0 \tag{4}$$

where W_t and W_0 are the weight of the HBCAs before and after oil uptake, respectively.

Reusability. The reusability of the HBCAs was evaluated by three steps. (1) Compression: The absorbed solvent was removed by compressing the aerogels between parallel glass slides whereby >90% strain was applied. The weight of the aerogels after compression during each cycle was measured to ensure that more than 90% of the absorbed solvent was removed. (2) Rinsing: The compressed HBCAs were rinsed three times with 20 mL of *tert*-butanol to swell the samples back to their initial shape and remove the residual absorbed solvent. (3) Freeze-drying: Gels were precooled for 2 h at −20 °C followed by freeze-drying for 3 h to obtain the dried HBCAs. Then, the dried samples were weighed and used as oil-absorbing materials again.

RESULTS AND DISCUSSION

Infrared Spectroscopy. ATR-FTIR spectra of the samples are presented in Figure 2. Trimethylsilyl groups, abundant in TMCS (agent for hydrophobization of cellulose) but not present in cellulose, are distinguishable marker. After modification with TMCS, the vibrations characteristic of the CH_3 of silane was identified at 2970 cm^{-1} (ν(C−H)) and 750 cm^{-1} (δ(C−H)).[14,61] Moreover, Si−CH_3 bending at 1254 cm^{-1} and Si−C stretching at 840 and 870 cm^{-1} were obvious.[62] The intensity of these bands increased with the increased amount of chlorosilane in the reaction. While the O−H stretching at 3400 cm^{-1} did not vary obviously, which means the amount of hydroxyl group (−OH) of the bacterial cellulose has no

DOI: 10.1021/acsami.5b00846
ACS Appl. Mater. Interfaces 2015, 7, 7373−7381

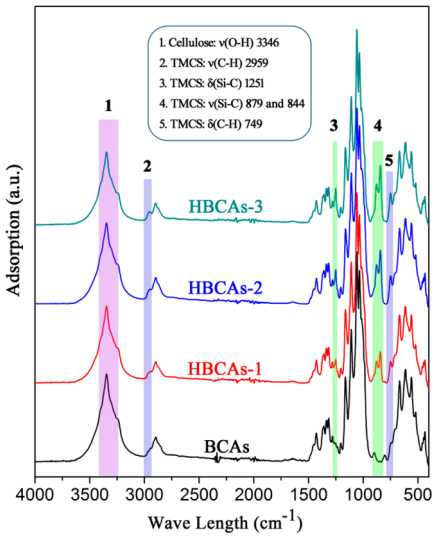

Figure 2. ATR-FTIR spectra of BCA, HBCA-1, HBCA-2, and HBCA-3.

significant change. Hence, the TMCS may not react with the abundant hydroxyl group in the interior of the cellulose nanofibers, and the degrees of substitution (DS) is in a low range.[51,54] The strong peaks of pyranose ring stretching between 1100 and 1000 cm^{-1} were also unchanged, and these peaks hid the weak peaks of Si−O−C stretching.

EDX Spectra and DS. The EDX spectra (Figure 3) were performed to investigate the trimethylsilylation of bacterial

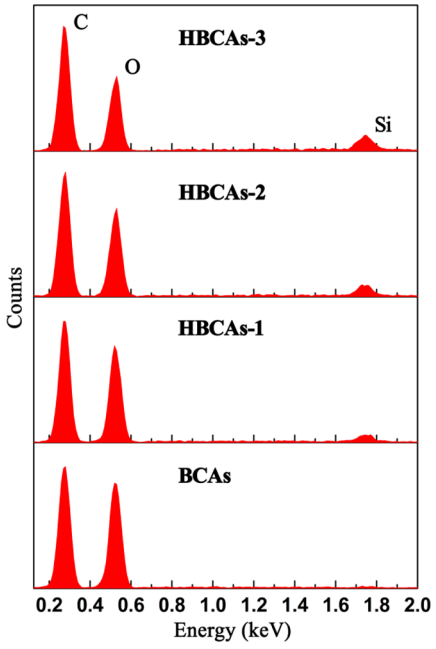

Figure 3. EDX spectra of BCA, HBCA-1, HBCA-2, and HBCA-3.

cellulose. The BCAs display the carbon and oxygen peaks, no silicon peak. Besides the carbon and oxygen peaks, the silicon peak appears in the EDX spectra of HBCAs after trimethylsilylation. These elements' atomic percentage could be calculated by element analysis (Table S1, Supporting Information). With the increase of modifier concentration, the carbon content increased from 53.82 to 54.92% when the silicon increased to 1.13%, while the oxygen content decreased from 46.18 to 43.95%. Which can be attributed to that there are three methyl groups ($-CH_3$) without oxygen in every TMCS molecular.

Herein, the modifier with only one active group instead of the modifier (e.g., titanium isopropoxide,[15,48] methyltrimethoxysilane,[14] methyltrichlorosilane,[63] etc.) contains three or four active groups is used to accomplish the hydrophobization of cellulose aerogels or the similar chitin aerogels. Then, the modifier (TMCS) molecules will not condense with each other modifier once they react with the hydroxyl group of the bacterial cellulose. This makes it possible to employ the contents of Si to evaluate the DS of HBCAs. The proportion of carbon, oxygen, and silicon could be detected by EDX spectra. Based on the proportion of the relative elements, the DS was calculated as according to eq 5:

$$\mathrm{DS} = \frac{N_{r(OH)}}{N_{(C_6H_{10}O_5)}} = \frac{N_{Si}}{(N_C - 3N_{Si})/6} = \frac{C_{Si}}{(C_C - 3C_{Si})/6} \quad (5)$$

where $N_{r(OH)}$ represents the amount of hydroxyl group which has reacted with TMCS in cellulose; $N_{(C_6H_{10}O_5)}$ represents the amount of anhydroglucose unit of cellulose; and N_C and N_{Si} represent the amount of carbon atom and silica atom in the HBCAs, respectively. C_C and C_{Si} are the atomic percentage of carbon and silica, respectively.

As shown in Table 2, the DS of the samples is varying from zero to 0.132. Based on the theory of Heux et al. that the

Table 2. DS, Density, and BET Surface Area of Aerogel Samples

sample	DS	density (mg/cm^3)	BET surface area (m^2/g)
BCA	0	6.74 ± 0.21	160.2
HBCA-1	0.075	6.69 ± 0.27	169.1
HBCA-2	0.114	6.77 ± 0.18	180.7
HBCA-3	0.132	6.75 ± 0.22	179.3

modification just occurs on the surface of cellulose nanofibers when the DS less than 0.4,[51] it could be concluded that only the surface molecule chains of the cellulose nanofibers in BCA are reacted with TMCS.

Morphology. As presented in Figure 1, both the macromorphology of BCA before and after trimethylsilylation were white and regular cuboid. This indicated that the trimethylsilyl modification did little affect the shape of BCA.

On a micro level, a web-like structure of BCA consists of disorderly and dispersive nanometer-sized cellulose nanofibers (Figure 4). After trimethylsilylation, the web-like structure was fully retained. Moreover, the apparent diameter of the nanofibers of all the samples was in the range of 20−80 nm. Compared with the cellulose nanofibers of BCA, the nanofibers of HBCAs was not wider. This phenomenon is quite different with the esterification of cellulose microfibrils with palmitoyl chloride. This could be understood as that the size of the modifier (i.e., TMCS) is much smaller than palmitoyl chloride. In addition, based on the research of Heux et al.,[50,51] higher DS increase the width of cellulose nanofibers more obviously due to the incorporation of the modifier. Consequently, no lateral expansion is observed in this work means that the trimethylsilylation does not occur in the interior of the cellulose nanofibers and the DS will be restricted to low values. The low DS is beneficial to preserve the mechanical

DOI: 10.1021/acsami.5b00846
ACS Appl. Mater. Interfaces 2015, 7, 7373−7381

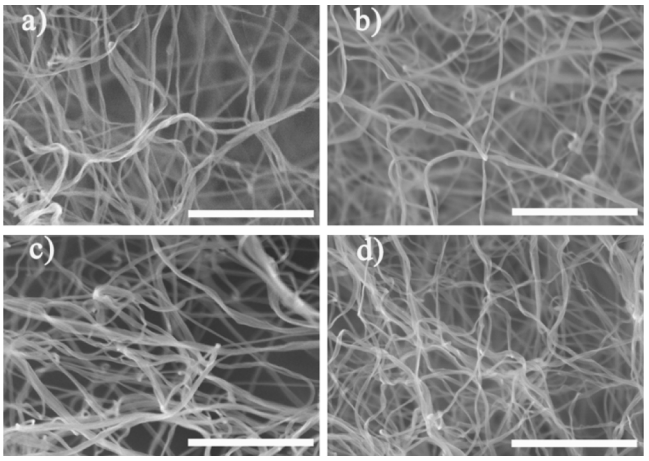

Figure 4. SEM images of (a) BCA, (b) HBCA-1, (c) HBCA-2, and (d) HBCA-3. The scale bar is 1 μm.

properties of cellulose nanofibers as few damages to the fibers and the crossing points. Hence, BCA could keep its original macroscopic shape after the trimethylsilylation in the mild reaction condition.

Density, BET Surface Area, and Porosity. As shown in Table 2, the density of the HBCAs was similar to the density of BCA, no obvious increase, because the DS is too low to affect the bulk density of cellulose aerogels in this work. While the amount of nitrogen physisorption (Figure S1, Supporting Information) and the BET surface area (Table 2) of the cellulose aerogel samples increased slightly. A possible explanation is that the TMCS roughened the surface of bacterial cellulose nanofibers through the trimethylsilylation. The porosity of BCAs was about 99.6% which was calculated according to eq 1. Because the DS is much too low, the density and the microstructure of BCA are not changed obviously after the trimethylsilylation, and thus, it is reasonable to believe that the porosity is constant through the trimethylsilylation process. Hence, like that of BCA, the approximate porosity of the HBCAs was 99.6%.

XRD. The XRD patterns of BCA and HBCAs are shown in Figure 5. Crystallographically, bacterial cellulose had the cellulose-I structure. The peaks shown corresponded to the diffraction planes of $1\bar{1}0$, 110 and 200, respectively.[64] Compared with BCA, no peak shifting or appearance of new peaks was observed in the XRD patterns of HBCAs. This indicated that the trimethylsilylation of BCA did not generate a new phase.

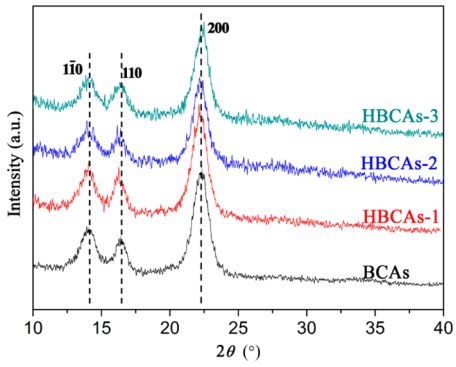

Figure 5. XRD spectra of the cellulose aerogel samples.

The crystallinity (χ_c), which was calculated based on the crystalline and amorphous intensity of cellulose aerogels, is calculated following the method in ref 60. It was found that the crystallinity has a slight decrease (Table 3). Nevertheless, the

Table 3. χ_c, L_{200}, and d_{200} of Cellulose Aerogel Samples

sample	χ_c (%)	L_{200} (Å)	d_{200} (Å)[a]
BCA	83.2	65.4	3.98
HBCA-1	80.7	63.2	3.97
HBCA-2	80.1	66.7	3.97
HBCA-3	79.8	65.8	3.98

[a]The d_{200} values were calculated following Bragg's law.

crystallite size of reflection (L_{200}) and the interlayer distance (d_{200}) of BCA and HBCAs of these cellulose aerogel samples did not show obvious variation after the trimethylsilylation (Table 3). This may be because the modifier (TMCS) on the surface of cellulose nanofibers enhanced the proportion of amorphous phase, while the trimethylsilylation did not destroy the crystal structure of bacterial cellulose. The increase of amorphous phase did not damage the crystalline phase, which can further suggest that the trimethylsilylation of BCA with TMCS occurred essentially only on the surface of the cellulose nanofibers.

Thermal Degradation Behavior. The TGA and DTG curves of BCA and the HBCAs are shown in Figure 6. Compared with the original cellulose aerogel, the TGA curves

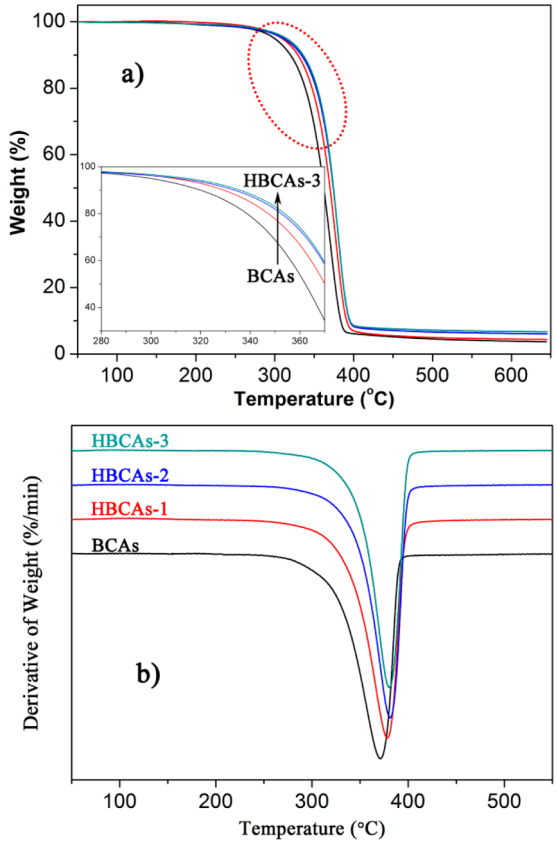

Figure 6. (a) Thermogravimetry analysis (TGA) and (inset) magnification of the part circled by dotted line, and (b) derivative thermogravimetry (DTG) curves of BCA, HBCA-1, HBCA-2, and HBCA-3.

DOI: 10.1021/acsami.5b00846
ACS Appl. Mater. Interfaces 2015, 7, 7373−7381

(Figure 6a) of trimethylsilylated cellulose aerogels exhibit a certain difference. The thermal decomposition of cellulose is known to be promoted by the modification of organic acids and acyl chloride (e.g., acetic acid, dodecanoic acid, *p*-toluenesulfonyl chloride, oleic acid, stearic acid, etc.). The decomposition temperature is lower when the longer carbon chain of modifier is used. Bismarck et al.[60] ascribed this to the reduced number of effective hydrogen bonds between cellulose nanofibers, as the nanofibers can then not be closely packed. In contrast, the decomposition temperature of BCAs had a slight enhancement after the trimethylsilylation, and the higher DS endowed the sample with a higher decomposition temperature (shifted from 370 to 380 °C, Figure 6b). This observation shows that the modifier (TMCS) has a stabilizing effect on bacterial cellulose. The similar stabilizing effect is also demonstrated in cellulose-silica composite aerogels.[59,65,66] Silica could raise the decomposition temperature of cellulose. Compared with silica, the TMCS has the same silicon, and Si−O bond will also form after it reacts with cellulose. Hence, the silicon and Si−O bond maybe significant to improve the thermal stability of cellulose.

Mechanical Properties. The compressive stress−strain curves of BCAs and HBCAs are presented in Figure 7. These

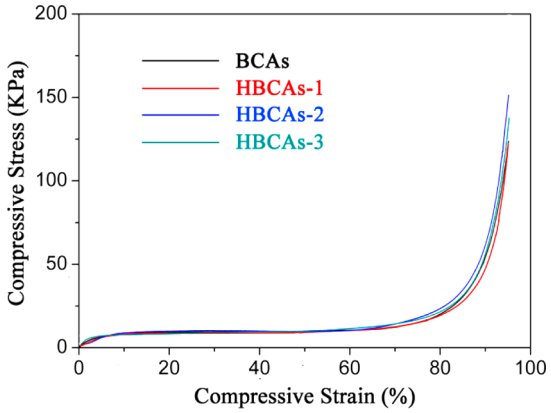

Figure 7. Compressive stress−strain curves of BCA, HBCA-1, HBCA-2, and HBCA-3.

curves may be separated into two regions: a very slowly increasing stress response below 70% strain and an exponentially increasing stress response above 70% strain. At 70% strain, the compressive stress of cellulose aerogels was just about 12 kPa. Because the web-like ultrafine nanofibers could be preserved perfectly in the cellulose aerogels instead of being crushed into lamellar structure by ice crystal, the BCAs and HBCAs are flexible. Besides, the high porosity is also vital for the excellent flexibility. Over 70% strain, it will exhibit higher stress as most hollow parts have been compressed and the solid cellulose nanofibers will touch with each other to increase the compressive resistance. The difference between these curves are caused by the nonuniform compactness of the aerogels as they were produced by bacteria that were sensitive to the condition culture medium. The nonuniformity has little effect on the curves below 70% strain, while it was more obvious with higher compressive strain, which separates the overlapped curves.

Wettability. The wettability of the cellulose aerogels are shown in Figure 8. Droplets of water and gasoline were successively deposited on the upper surface of the BCAs and HBCAs blocks. Obviously, the BCAs displayed a strong amphiphilic character, as both the water and gasoline droplets

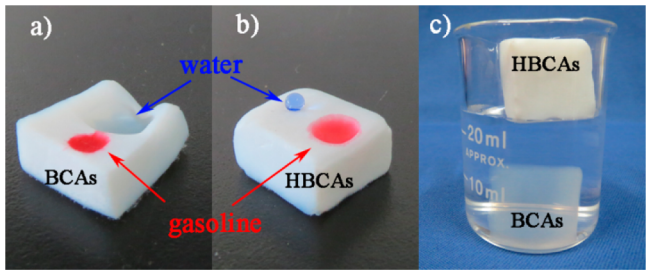

Figure 8. Water and gasoline were colored blue (Methyl Blue) and red (Oil Red), respectively, and dropped on the surface of (a) BCA and (b) HBCA-3. (c) The HBCA-3 floated on water, while BCA sank into water.

were instantaneously absorbed. In contrast, the gasoline immediately penetrated into the HBCAs, while water remained at the surface, demonstrating the combined hydrophobic and oleophilic properties of this material. The HBCAs displayed high contact angles (as high as 146.5°; Figure S2, Supporting Information), and the contact angles increased with the increase of DS. According to Wenzel's theory,[67,68] the wettability of solid surfaces is governed by both the chemical composition and the geometrical microstructure of the surface as. At thermodynamic equilibrium, the apparent contact angle of the sample surface and the roughness factor of the given surface have the relationship:

$$\cos \theta^{w} = r \cos \theta \quad (6)$$

where θ^{w} corresponds to the apparent contact angle, r represents the roughness factor, and θ refers to Young's angle. Herein, the surface energy of the cellulose was effectively decreased by the trimethylsilylation. Besides, the ultrafine cellulose nanofibers which could be preserved completely after the trimethylsilylation endow the HBCAs with high surface roughness. Hence, the contact angle measured on the surface was surprisingly high (137.1−146.5°) even at very low DS (0.075−0.132). Compared with most hydrophobic cellulose aerogels,[14,15,48] the water contact angles of the samples in this work are higher. This may be caused by the difference in their microstructure. In this work, the HBCAs consist of disorderly and dispersive nanometer-sized cellulose nanofibers, unlike the cellulose network formed by the connected lamella in the relative literature.[14,15,48] Hence, the HBCAs will possess higher roughness and then show higher water contact angle.

The BCAs absorbed water and sank to the bottom immediately when it was transferred to the surface of water (Figure 8c). On the contrary, the HBCAs could float on the surface of water owing to the hydrophobicity and ultralight weight. The unique wettability of the HBCAs means that they have the potential to be used as oil/water separation material.

Superabsorption Capacity. As shown in Figure 9, plant oil and chloroform were dropped at the surface and bottom of water, respectively. The HBCAs selectively absorbed the plants oil and chloroform from water, and the oil-filled HBCAs could be separated from water expediently (Movies S1 and S2, Supporting Information) owing to the excellent mechanical properties which make sure their integrity (Supporting Information). By contrast, the BCA quickly saturated with both water and plant oil, and it lost the oil-absorbing capability once wetted by water (Movie S3, Supporting Information).

The absorption performance of HBCAs for different oils and organic solvents was further investigated (Figure 10a). From

DOI: 10.1021/acsami.5b00846
ACS Appl. Mater. Interfaces 2015, 7, 7373−7381

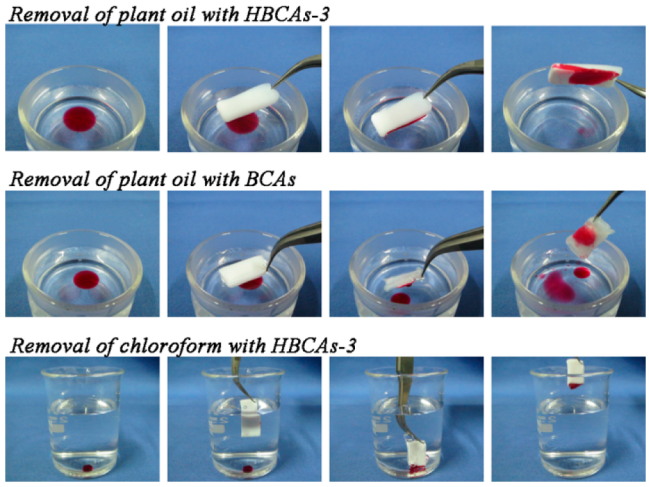

Figure 9. Removal of a red-colored plant oil spill (15 μL) from water with the slices (ca. 20 × 8 × 2) of (top row) HBCAs and (middle row) BCA; (bottom row) removal of chloroform from the bottom of water with the slice of HBCAs.

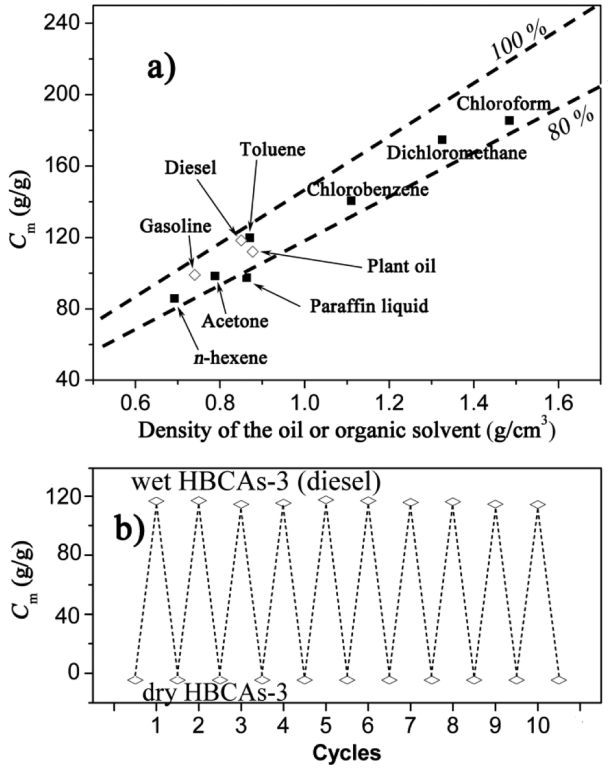

Figure 10. (a) Plot of the mass-based absorption capacity for different organic solvents and oils as a function of the density of the liquid. The upper dashed line represents the theoretical volume-based absorption capacity (v/v) corresponding to the case where aerogel is nominally completely filled with the oils or organic liquids, and the lower one dashed line represents the case where it is 80% filled. (b) Demonstration of the reusability of HBCA-3 as an oil absorbent. The absorption capacity (C_m) with regard to diesel was evaluated after up to 10 rinsing–absorption cycles.

the absorption kinetics (Figure S3, Supporting Information), it is found that the samples need about 20 s to reach absorption equilibrium in paraffin liquid and plant oil, while they need just about 12 s in the other oils or organic solvents. Because the viscosity significantly affects the movement velocity of oil molecules, it takes different time to achieve the absorption equilibrium.[20,63] The mass-based maximum absorption capacities C_m for the oils were 86 to 185 g/g (Figure 10a). Generally, the value of C_m is relevant to the density of the liquid, and it increases with the density of the liquid. Compared with the reported hydrophobic cellulose aerogels, the C_m value was enhanced significantly, likely because the high porosity, high surface area, and ultralow density of BCA were preserved very well and did not obviously affected by the modifier in this work. On the contrary, the preparation methods reported in the literature made these parameters of cellulose aerogels were remarkably affected by the modifier, especially the density. For example, the bulk density of the silylated cellulose aerogels is twice as much as the pure cellulose aerogels when the water contact angle achieve 136° in the work of Tingaut et al.[14] Because the volume-based absorption capacity is significant for oil-absorbing materials, described by Ikkala et al.,[15] it was investigated in this work (Figure 10a). It was found that the volume-based absorption capacities of the HBCAs reached over 80%. This means that almost all of the hollow parts were crammed by the oils/organics.

To test the reusability, the HBCAs contain diesel were treated as three steps, which have been amply described in the Experimental Section, to thoroughly remove the diesel. Then, the HBCAs were used to absorb oil again. The cleaning–absorption cycle was performed 10 times, and the C_m value maintained at nearly 120 g/g after each cycle (Figure 10b). Moreover, the macro-morphology of the HBCAs remained unchanged. This means that the HBCAs have the potential to be recycled. The compressive stress–strain curves (Figure S4, Supporting Information), and the relative mechanical properties of oil-filled HBCAs have been discussed in the Supporting Information.

CONCLUSIONS

Surface-only modification of the 3D web-like skeleton of BCAs was accomplished via a feasible liquid-phase reaction followed by freeze-drying to obtain HBCAs without shape and microstructure change. In this process, the hydroxyl groups in the surface molecule chains of the cellulose nanofibers took part in the trimethylsilylation with TMCS. Then, the surface energy of the cellulose nanofibers was decreased effectively. Furthermore, the 3D web-like microstructure, which was comprised of ultrathin (20–80 nm) cellulose nanofibers, was maintained because of the very low DS (≤0.132) of the HBCAs. Hence, the high roughness and low surface energy endowed the HBCAs with hydrophobic and oleophilic properties, and highly selective absorption of oils and nonpolar liquids. Moreover, the surface-only modification of BCAs made sure that the low density (≤6.77 mg/cm^3), high surface area (≥169.1 m^2/g), and high porosity (≈ 99.6%) were well preserved in the HBCAs. Accordingly, the HBCAs exhibited high mass absorption capacities for a wide variety of oils and organic solvents (up to 185 g/g). This means that the HBCAs are wonderful candidates for oil adsorption. In conclusion, the surface only trimethylsilylation of BCA for oil absorbents was achieved, which provided another way to multifunctionalize cellulose aerogels in addition to CVD method.

ASSOCIATED CONTENT

Supporting Information

Elements atomic percentage calculated by element analysis from EDX spectra; nitrogen adsorption–desorption isotherms

DOI: 10.1021/acsami.5b00846
ACS Appl. Mater. Interfaces 2015, 7, 7373–7381

and images of contact angle measurements of BCA and HBCAs; absorption kinetic curves of different oils and organic sorbents; compressive stress−strain curves of oil-filled HBCAs-3 and the relative analysis of the mechanical properties of oil-filled HBCAs-3; and movies showing the removal of plant oil with HBCAs-3 from water surface, removal of chloroform with HBCAs-3 from the bottom of water, and removal of plant oil with BCAs from water surface. This material is available free of charge via the Internet at http://pubs.acs.org.

AUTHOR INFORMATION

Corresponding Author

*E-mail: xiangjh@ucas.ac.cn.

Author Contributions

†These authors contributed equally to this work.

Notes

The authors declare no competing financial interest.

ACKNOWLEDGMENTS

This work is supported by the National Basic Research Program of China (973 Program; no. 2011CB706900) the National Nature Science Foundation of China (nos. 50872149 and 50502003), the Scientific Research Foundation for Returned Scholars within the Ministry of Education of China, and the President Foundation of the Graduate University of the Chinese Academy of Sciences.

REFERENCES

(1) Schrope, M. Oil Spill: Deep Wounds. *Nature* **2011**, *472*, 152−154.

(2) Jernelov, A. How to Defend against Future Oil Spills. *Nature* **2010**, *466*, 182−183.

(3) Schrope, M. Researchers Debate Oil-Spill Remedy. *Nature* **2013**, *493*, 461.

(4) Barbier, E. B.; Moreno-Mateos, D.; Rogers, A. D.; Aronson, J.; Pendleton, L.; Danovaro, R.; Henry, L.-A.; Morato, T.; Ardron, J.; Dover, C. L. V. Protect the Deep Sea. *Nature* **2014**, *505*, 475−177.

(5) Wang, F.; Lei, S.; Xue, M.; Ou, J.; Li, W. In Situ Separation and Collection of Oil from Water Surface Via a Novel Superoleophilic and Superhydrophobic Oil Containment Boom. *Langmuir* **2014**, *30*, 1281−1289.

(6) Brown, P. S.; Atkinson, O. D. L. A.; Badyal, J. P. S. Ultrafast Oleophobic−Hydrophilic Switching Surfaces for Antifogging, Self-Cleaning, and Oil−Water Separation. *ACS Appl. Mater. Interfaces* **2014**, *6*, 7504−7511.

(7) Liu, N.; Chen, Y.; Lu, F.; Cao, Y.; Xue, Z.; Li, K.; Feng, L.; Wei, Y. Straightforward Oxidation of a Copper Substrate Produces an Underwater Superoleophobic Mesh for Oil/Water Separation. *ChemPhysChem* **2013**, *14*, 3489−3494.

(8) Avila, A. F.; Munhoz, V. C.; de Oliveira, A. M.; Santos, M. C. G.; Lacerda, G. R. B. S.; Gonçalves, C. P. Nano-Based Systems for Oil Spills Control and Cleanup. *J. Hazard. Mater.* **2014**, *272*, 20−27.

(9) Cortese, B.; Caschera, D.; Federici, F.; Ingo, G. M.; Gigli, G. Superhydrophobic Fabrics for Oil−Water Separation through a Diamond Like Carbon (DLC) Coating. *J. Mater. Chem. A* **2014**, *2*, 6781−6789.

(10) Wang, F.; Lei, S.; Xue, M.; Ou, J.; Li, C.; Li, W. Superhydrophobic and Superoleophilic Miniature Device for the Collection of Oils from Water Surfaces. *J. Phys. Chem. C* **2014**, *118*, 6344−6351.

(11) Zhang, F.; Zhang, W. B.; Shi, Z.; Wang, D.; Jin, J.; Jiang, L. Nanowire-Haired Inorganic Membranes with Superhydrophilicity and Underwater Ultralow Adhesive Superoleophobicity for High-Efficiency Oil/Water Separation. *Adv. Mater.* **2013**, *25*, 4192−4198.

(12) Cao, Y.; Zhang, X.; Tao, L.; Li, K.; Xue, Z.; Feng, L.; Wei, Y. Mussel-Inspired Chemistry and Michael Addition Reaction for Efficient Oil/Water Separation. *ACS Appl. Mater. Interfaces* **2013**, *5*, 4438−4442.

(13) Pavía-Sanders, A.; Zhang, S.; Flores, J. A.; Sanders, J. E.; Raymond, J. E.; Wooley, K. L. Robust Magnetic/Polymer Hybrid Nanoparticles Designed for Crude Oil Entrapment and Recovery in Aqueous Environments. *ACS Nano* **2013**, *7*, 7552−7561.

(14) Zhang, Z.; Sèbe, G.; Rentsch, D.; Zimmermann, T.; Tingaut, P. Ultralightweight and Flexible Silylated Nanocellulose Sponges for the Selective Removal of Oil from Water. *Chem. Mater.* **2014**, *26*, 2659−2668.

(15) Korhonen, J. T.; Kettunen, M.; Ras, R. H. A.; Ikkala, O. Hydrophobic Nanocellulose Aerogels as Floating, Sustainable, Reusable, and Recyclable Oil Absorbents. *ACS Appl. Mater. Interfaces* **2011**, *3*, 1813−1816.

(16) Wu, Z.-Y.; Li, C.; Liang, H.-W.; Zhang, Y.-N.; Wang, X.; Chen, J.-F.; Yu, S.-H. Carbon Nanofiber Aerogels for Emergent Cleanup of Oil Spillage and Chemical Leakage under Harsh Conditions. *Sci. Rep.* **2014**, *4*.

(17) Ruan, C.; Ai, K.; Li, X.; Lu, L. A Superhydrophobic Sponge with Excellent Absorbency and Flame Retardancy. *Angew. Chem., Int. Ed.* **2014**, *53*, 5556−5560.

(18) Zhu, Q.; Pan, Q. Mussel-Inspired Direct Immobilization of Nanoparticles and Application for Oil−Water Separation. *ACS Nano* **2014**, *8*, 1402−1409.

(19) Zhu, Q.; Chu, Y.; Wang, Z.; Chen, N.; Lin, L.; Liu, F.; Pan, Q. Robust Superhydrophobic Polyurethane Sponge as a Highly Reusable Oil-Absorption Material. *J. Mater. Chem. A* **2013**, *1*, 5386−5393.

(20) Pan, Y.; Shi, K.; Peng, C.; Wang, W.; Liu, Z.; Ji, X. Evaluation of Hydrophobic Polyvinyl-Alcohol Formaldehyde Sponges as Absorbents for Oil Spill. *ACS Appl. Mater. Interfaces* **2014**, *6*, 8651−8659.

(21) Zhao, X.; Li, L.; Li, B.; Zhang, J.; Wang, A. Durable Superhydrophobic/Superoleophilic PDMS Sponges and Their Applications in Selective Oil Absorption and in Plugging Oil Leakages. *J. Mater. Chem. A* **2014**, *2*, 18281−18287.

(22) Jing, P.; Fang, X.; Yan, J.; Guo, J.; Fang, Y. Ultra-Low Density Porous Polystyrene Monolith: Facile Preparation and Superior Application. *J. Mater. Chem. A* **2013**, *1*, 10135−10141.

(23) Choi, S.-J.; Kwon, T.-H.; Im, H.; Moon, D.-I.; Baek, D. J.; Seol, M.-L.; Duarte, J. P.; Choi, Y.-K. A Polydimethylsiloxane (PDMS) Sponge for the Selective Absorption of Oil from Water. *ACS Appl. Mater. Interfaces* **2011**, *3*, 4552−4556.

(24) Yang, Y.; Deng, Y.; Tong, Z.; Wang, C. Multifunctional Foams Derived from Poly(melamine formaldehyde) as Recyclable Oil Absorbents. *J. Mater. Chem. A* **2014**, *2*, 9994−9999.

(25) Zhu, X.; Zhang, Z.; Ren, G.; Yang, J.; Wang, K.; Xu, X.; Men, X.; Zhou, X. A Novel Superhydrophobic Bulk Material. *J. Mater. Chem.* **2012**, *22*, 20146−20148.

(26) Xue, Z.; Cao, Y.; Liu, N.; Feng, L.; Jiang, L. Special Wettable Materials for Oil/Water Separation. *J. Mater. Chem. A* **2014**, *2*, 2445−2460.

(27) Ceylan, D.; Dogu, S.; Karacik, B.; Yakan, S. D.; Okay, O. S.; Okay, O. Evaluation of Butyl Rubber as Sorbent Material for the Removal of Oil and Polycyclic Aromatic Hydrocarbons from Seawater. *Environ. Sci. Technol.* **2009**, *43*, 3846−3852.

(28) Gui, X.; Zeng, Z.; Lin, Z.; Gan, Q.; Xiang, R.; Zhu, Y.; Cao, A.; Tang, Z. Magnetic and Highly Recyclable Macroporous Carbon Nanotubes for Spilled Oil Sorption and Separation. *ACS Appl. Mater. Interfaces* **2013**, *5*, 5845−5850.

(29) Rajaković-Ognjanović, V.; Aleksić, G.; Rajaković, L. Governing Factors for Motor Oil Removal from Water with Different Sorption Materials. *J. Hazard. Mater.* **2008**, *154*, 558−563.

(30) Rajakovic, V.; Aleksic, G.; Radetic, M.; Rajakovic, L. Efficiency of Oil Removal from Real Wastewater with Different Sorbent Materials. *J. Hazard. Mater.* **2007**, *143*, 494−499.

(31) Teas, C.; Kalligeros, S.; Zanikos, F.; Stournas, S.; Lois, E.; Anastopoulos, G. Investigation of the Effectiveness of Absorbent Materials in Oil Spills Clean Up. *Desalination* **2001**, *140*, 259−264.

DOI: 10.1021/acsami.5b00846
ACS Appl. Mater. Interfaces 2015, 7, 7373−7381

(32) Choi, H. M.; Cloud, R. M. Natural Sorbents in Oil Spill Cleanup. *Environ. Sci. Technol.* **1992**, *26*, 772−776.
(33) Moriwaki, H.; Kitajima, S.; Kurashima, M.; Hagiwara, A.; Haraguchi, K.; Shirai, K.; Kanekatsu, R.; Kiguchi, K. Utilization of Silkworm Cocoon Waste as a Sorbent for the Removal of Oil from Water. *J. Hazard. Mater.* **2009**, *165*, 266−270.
(34) Radetic, M.; Ilic, V.; Radojevic, D.; Miladinovic, R.; Jocic, D.; Jovancic, P. Efficiency of Recycled Wool-Based Nonwoven Material for the Removal of Oils from Water. *Chemosphere* **2008**, *70*, 525−530.
(35) Wu, B.; Zhou, M. H. Recycling of Waste Tyre Rubber into Oil Absorbent. *Waste Manage.* **2009**, *29*, 355−359.
(36) Wu, J.; Wang, N.; Wang, L.; Dong, H.; Zhao, Y.; Jiang, L. Electrospun Porous Structure Fibrous Film with High Oil Adsorption Capacity. *ACS Appl. Mater. Interfaces* **2012**, *4*, 3207−3212.
(37) Lin, J.; Tian, F.; Shang, Y.; Wang, F.; Ding, B.; Yu, J.; Guo, Z. Co-Axial Electrospun Polystyrene/Polyurethane Fibres for Oil Collection from Water Surface. *Nanoscale* **2013**, *5*, 2745−2755.
(38) Wu, Z.-Y.; Li, C.; Liang, H.-W.; Chen, J.-F.; Yu, S.-H. Ultralight, Flexible, and Fire-Resistant Carbon Nanofiber Aerogels from Bacterial Cellulose. *Angew. Chem., Int. Ed.* **2013**, *52*, 2925−2929.
(39) Yu, Y.; Wu, X.; Guo, D.; Fang, J. Preparation of Flexible, Hydrophobic, and Oleophilic Silica Aerogels Based on a Methyltriethoxysilane Precursor. *J. Mater. Sci.* **2014**, *49*, 7715−7722.
(40) Gurav, J. L.; Rao, A. V.; Nadargi, D. Y.; Park, H.-H. Ambient Pressure Dried Teos-Based Silica Aerogels: Good Absorbents of Organic Liquids. *J. Mater. Sci.* **2010**, *45*, 503−510.
(41) Sun, H.; Xu, Z.; Gao, C. Multifunctional, Ultra-Flyweight, Synergistically Assembled Carbon Aerogels. *Adv. Mater.* **2013**, *25*, 2554−2560.
(42) Kabiri, S.; Tran, D. N. H.; Altalhi, T.; Losic, D. Outstanding Adsorption Performance of Graphene−Carbon Nanotube Aerogels for Continuous Oil Removal. *Carbon* **2014**, *80*, 523−533.
(43) Yang, X.; Cranston, E. D. Chemically Cross-Linked Cellulose Nanocrystal Aerogels with Shape Recovery and Superabsorbent Properties. *Chem. Mater.* **2014**, *26*, 6016−6025.
(44) Sehaqui, H.; Zhou, Q.; Berglund, L. A. High-Porosity Aerogels of High Specific Surface Area Prepared from Nanofibrillated Cellulose (NFC). *Compos. Sci. Technol.* **2011**, *71*, 1593−1599.
(45) Aulin, C.; Netrval, J.; Wagberg, L.; Lindstrom, T. Aerogels from Nanofibrillated Cellulose with Tunable Oleophobicity. *Soft Matter* **2010**, *6*, 3298−3305.
(46) Sehaqui, H.; Salajkova, M.; Zhou, Q.; Berglund, L. A. Mechanical Performance Tailoring of Tough Ultra-High Porosity Foams Prepared from Cellulose I Nanofiber Suspensions. *Soft Matter* **2010**, *6*, 1824−1832.
(47) Paakko, M.; Vapaavuori, J.; Silvennoinen, R.; Kosonen, H.; Ankerfors, M.; Lindstrom, T.; Berglund, L. A.; Ikkala, O. Long and Entangled Native Cellulose I Nanofibers Allow Flexible Aerogels and Hierarchically Porous Templates for Functionalities. *Soft Matter* **2008**, *4*, 2492−2499.
(48) Kettunen, M.; Silvennoinen, R. J.; Houbenov, N.; Nykänen, A.; Ruokolainen, J.; Sainio, J.; Pore, V.; Kemell, M.; Ankerfors, M.; Lindström, T.; Ritala, M.; Ras, R. H. A.; Ikkala, O. Photoswitchable Superabsorbency Based on Nanocellulose Aerogels. *Adv. Funct. Mater.* **2011**, *21*, 510−517.
(49) Cervin, N.; Aulin, C.; Larsson, P.; Wågberg, L. Ultra Porous Nanocellulose Aerogels as Separation Medium for Mixtures of Oil/Water Liquids. *Cellulose* **2012**, *19*, 401−410.
(50) Berlioz, S.; Molina-Boisseau, S.; Nishiyama, Y.; Heux, L. Gas-Phase Surface Esterification of Cellulose Microfibrils and Whiskers. *Biomacromolecules* **2009**, *10*, 2144−2151.
(51) Fumagalli, M.; Ouhab, D.; Boisseau, S. M.; Heux, L. Versatile Gas-Phase Reactions for Surface to Bulk Esterification of Cellulose Microfibrils Aerogels. *Biomacromolecules* **2013**, *14*, 3246−3255.
(52) Missoum, K.; Belgacem, M.; Bras, J. Nanofibrillated Cellulose Surface Modification: A Review. *Materials* **2013**, *6*, 1745−1766.
(53) Kim, D.-Y.; Nishiyama, Y.; Kuga, S. Surface Acetylation of Bacterial Cellulose. *Cellulose* **2002**, *9*, 361−367.
(54) Ifuku, S.; Nogi, M.; Abe, K.; Handa, K.; Nakatsubo, F.; Yano, H. Surface Modification of Bacterial Cellulose Nanofibers for Property Enhancement of Optically Transparent Composites: Dependence on Acetyl-Group DS. *Biomacromolecules* **2007**, *8*, 1973−1978.
(55) Nogi, M.; Abe, K.; Handa, K.; Nakatsubo, F.; Ifuku, S.; Yano, H. Property Enhancement of Optically Transparent Bionanofiber Composites by Acetylation. *Appl. Phys. Lett.* **2006**, *89*, 233123.
(56) Lee, K.-Y.; Blaker, J. J.; Bismarck, A. Surface Functionalisation of Bacterial Cellulose as the Route to Produce Green Polylactide Nanocomposites with Improved Properties. *Compos. Sci. Technol.* **2009**, *69*, 2724−2733.
(57) Freire, C. S. R.; Silvestre, A. J. D.; Neto, C. P.; Belgacem, M. N.; Gandini, A. Controlled Heterogeneous Modification of Cellulose Fibers with Fatty Acids: Effect of Reaction Conditions on the Extent of Esterification and Fiber Properties. *J. Appl. Polym. Sci.* **2006**, *100*, 1093−1102.
(58) Jin, H.; Kettunen, M.; Laiho, A.; Pynnönen, H.; Paltakari, J.; Marmur, A.; Ikkala, O.; Ras, R. H. A. Superhydrophobic and Superoleophobic Nanocellulose Aerogel Membranes as Bioinspired Cargo Carriers on Water and Oil. *Langmuir* **2011**, *27*, 1930−1934.
(59) Sai, H.; Xing, L.; Xiang, J.; Cui, L.; Jiao, J.; Zhao, C.; Li, Z.; Li, F. Flexible Aerogels Based on an Interpenetrating Network of Bacterial Cellulose and Silica by a Non-Supercritical Drying Process. *J. Mater. Chem. A* **2013**, *1*, 7963−7970.
(60) Lee, K.-Y.; Quero, F.; Blaker, J.; Hill, C. S.; Eichhorn, S.; Bismarck, A. Surface Only Modification of Bacterial Cellulose Nanofibres with Organic Acids. *Cellulose* **2011**, *18*, 595−605.
(61) Taajamaa, L.; Kontturi, E.; Laine, J.; Rojas, O. J. Bicomponent Fibre Mats with Adhesive Ultra-Hydrophobicity Tailored with Cellulose Derivatives. *J. Mater. Chem.* **2012**, *22*, 12072−12082.
(62) Andresen, M.; Johansson, L.-S.; Tanem, B. S.; Stenius, P. Properties and Characterization of Hydrophobized Microfibrillated Cellulose. *Cellulose* **2006**, *13*, 665−677.
(63) Duan, B.; Gao, H.; He, M.; Zhang, L. Hydrophobic Modification on Surface of Chitin Sponges for Highly Effective Separation of Oil. *ACS Appl. Mater. Interfaces* **2014**, *6*, 19933−19942.
(64) Jiang, F.; Hsieh, Y.-L. Super Water Absorbing and Shape Memory Nanocellulose Aerogels from Tempo-Oxidized Cellulose Nanofibrils via Cyclic Freezing−Thawing. *J. Mater. Chem. A* **2014**, *2*, 350−359.
(65) Cai, J.; Liu, S.; Feng, J.; Kimura, S.; Wada, M.; Kuga, S.; Zhang, L. Cellulose−Silica Nanocomposite Aerogels by in Situ Formation of Silica in Cellulose Gel. *Angew. Chem., Int. Ed.* **2012**, *51*, 2076−2079.
(66) Sai, H.; Xing, L.; Xiang, J.; Cui, L.; Jiao, J.; Zhao, C.; Li, Z.; Li, F.; Zhang, T. Flexible Aerogels with Interpenetrating Network Structure of Bacterial Cellulose-Silica Composite from Sodium Silicate Precursor via Freeze Drying Process. *RSC Adv.* **2014**, *4*, 30453−30461.
(67) Wenzel, R. N. Resistance of Solid Surfaces to Wetting by Water. *Ind. Eng. Chem.* **1936**, *28*, 988−994.
(68) Li, X. M.; Reinhoudt, D.; Crego-Calama, M. What Do We Need for a Superhydrophobic Surface? A Review on the Recent Progress in the Preparation of Superhydrophobic Surfaces. *Chem. Soc. Rev.* **2007**, *36*, 1350−1368.

DOI: 10.1021/acsami.5b00846
ACS Appl. Mater. Interfaces 2015, 7, 7373−7381